Large-activation-energy theory for premixed combustion under the influence of enthalpy fluctuations in the oncoming mixture Part I: general formulation

By X. Wu† AND P. Moin

1. Motivation and objectives

Premixed combustion in an enclosed chamber is susceptible to large-scale acoustic instability, which manifests as intense pressure fluctuations with predominant peaks at the characteristic acoustic frequencies of the combustor. Such an instability can occur in aero- and rocket engines as well as in land-based gas turbines (e.g., Harrje & Reardon 1972; Yu, Trouve & Daily 1991; Richards & Janus 1997). It has a number of detrimental effects. For example, the oscillatory load may lead to structural fatigue. The strong pressure fluctuation may cause flame flash-back and/or blow-off. These problems hinder the development of lean-burn gas turbine engines to reduce emissions of NO_X, because combustion in the lean limit is particularly prone to the instability. In practical applications, the instability has to be suppressed by passive (Schadow & Gutmark 1992) or active control (Candel 2002; Dowling & Morgans 2005).

It is generally recognized that combustion instability is essentially a self-excited oscillation sustained by a two-way coupling between the unsteady heat release and acoustic modes of the chamber (e.g., Poinsot *et al.* 1987; Langhorne 1988; Candel 2002). The unsteady heat release from the flame leads to amplification of acoustic pressure when the two are "in phase" according to Rayleigh's criterion. Acoustic fluctuations, on the other hand, may affect the flame and hence the heat release through kinematic, dynamic and chemo-thermal mechanisms, including:

(a) acoustic velocity advects the flame front;

(b) acoustic acceleration acts on the flame through the unsteady Rayleigh-Taylor (R-T) effect (Markstein 1953);

(c) acoustic pressure modifies the burning rate (e.g., McIntosh 1991);

(d) sound waves modulate the equivalence ratio of the mixture (Lieuwen & Zinn 1998).

The onset and control of combustion instability may be crucially affected by external disturbances. In an idealized model of a uniform oncoming flow of mixture, an arbitrary small-amplitude disturbance can be decomposed into acoustic, vortical and enthalpy modes. Based on this decomposition, it is natural to investigate the interaction of a flame with each of the three modes separately.

Theoretical modeling of combustion instability has mostly taken a semi-empirical approach, which seeks to establish the relations between the flame motion, heat release and external disturbances in a phenomenological manner (Lieuwen 2003; Ducruix *et al.* 2003). In particular, kinematic models based on the so-called G-equation, proposed by Fleifil *et al.* (1996), have been extended and used to describe the flame wrinkling caused

† Current Address: Department of Mathematics, Imperial College London, SW7 2BZ, U. K.

by acoustic (e.g., Dowling 1999; Schuller, Durox & Candel 2003), vortical (Baillot, Durox & Prud'hommr 1992) and enthalpy (Cho & Lieuwen 2005) perturbations. While some good predictions have been reported, it should be recognized that in this approach the flame is deprived of its internal thermal-diffusive structure and its intrinsic gas-expansion induced hydrodynamic field. As a result, the G-equation includes kinematic mechanism (a) only, while mechanisms (b) and (c) are completely beyond its scope.

An alternative approach, which seeks to describe flame-acoustic interactions on the basis of first principles, may be pursued by using the large-activation-energy asymptotic (AEA) approximations (Clavin 1994). Based on the assumptions of large Zeldovich number $\beta \gg 1$ and small Mach number $M \ll 1$, AEA was developed to characterize flame-flow interactions. Depending on the ratio of the characteristic length scale h^* of the flow motion to the flame thickness d (determined by thermal-chemical properties of the mixture), two distinguished regimes may arise. The "corrugate flamelet" regime occurs if $h^*/d \gg O(1)$, for which the flow-flame system acquires the well-known structure consisting of three zones: an $O(d/\beta)$ reaction zone an $O(d)$ preheat zone, and an $O(h^*)$ hydrodynamic zone (Pelce & Clavin 1982; Matalon & Matkowsky 1982, referred to as MM hereafter). The "thin-reaction-zone" regime resumes if $h^*/d \sim O(1)$, for which the preheat and hydrodynamic zones collapse so that a two-zoned structure emerges.

Using the AEA approach, several authors have investigated mechanism (c) referred to above. Harten, Kapila & Matkowsky (1984) considered the interaction of a flame with an acoustic wave, whose time scale is of $O(d/U_L)$, where U_L is the laminar flame speed. McIntosh (1991, 1993) analyzed the burning rate response to acoustic waves in several distinguished higher-frequency regimes. Clavin, Pelce & He (1990) studied the back effect of the change in the burning rate on the acoustic field, and showed that the closed-loop interaction leads to an exponential growth of the sound. Mechanism (b) was studied by Searby & Rochwerger (1991), who formulated the stability problem of a flame subjected to an externally prescribed acoustic pressure. Their calculations show that as the acoustic acceleration exceeds a threshold, it induces a violent subharmonic parametric instability. Pelce & Rochwerger (1992) analyzed the acoustic instability of a pre-existing stationary (slightly) curved flame, and showed that as the flame is perturbed, the unsteady heat release due to the surface-area change drives exponential growth of acoustic modes. However, the back effect of the latter on the flame was not considered.

The AEA theories for flame-acoustic interactions mentioned above were formulated either for one-way coupling or for two-way coupling in a special case. A general asymptotic theory was presented by Wu, Wang, Moin & Peters (2003) (referred to as WWMP hereafter) to describe the acoustic-flow-flame coupling in the "corrugated flamelet" regime. Using this general formulation, they provide a unified description of the flame-acoustic coupling mechanisms of Clavin *et al.* (1990) and Pelce & Rochwerger (1992). Recently, the general theory of WWMP was adapted by Wu & Law (2008) to study the impact of vortical disturbances on flame-acoustic coupling. Their analysis suggests that a small-amplitude vortical disturbance may initiate the subharmonic parametric resonance between the flame and the spontaneously generated sound wave. The resonant coupling may completely destabilize an otherwise intrinsically stable flame, causing an initially silent planar flame to evolve into a noisy and highly wrinkled state.

The present work is concerned with enthalpy disturbances, which may consist of both temperature and mass fraction (or equivalence ratio) fluctuations. The latter may arise due either to "unmixedness" of the oncoming fresh mixture (Shih, Lee & Santavicca 1996), or to combustion-generated acoustic waves interfering with the fuel-mixing section.

Its relevance in combustion instability was first recognized by Lieuwen & Zinn (1998), who proposed mechanism (d) mentioned earlier. Recent measurements indicate that pressure oscillations correlate strongly with the equivalence ratio fluctuation at the inlet (Zimmer & Tachibana 2007), and the latter was the primary contributor to the unsteady heat release that causes combustion instability (Lee, Kim & Santavicca 2000).

Enthalpy (equivalence ratio) disturbances are deliberately generated in active control systems using secondary fuel injection (e.g., Richards, Janus & Sobey 1999; Dowling & Morgans 2005), a control strategy believed to be most practical and efficient because of its flexible implementation and the sensitive response of the flame to enthalpy. In closed-loop control, modulating the fuel rate by a few percent may reduce the noise level by over 20 dB (Jones, Lee & Santavicca 1999). Surprisingly, however, there exist few theoretical and numerical studies of the interaction of a flame with enthalpy fluctuations. Cho & Lieuwen (2005) analyzed the linear response of a conical flame to equivalence ratio perturbation using the G-equation. Direct numerical simulations (DNS) were performed only recently by Birbaud *et al.* (2008) for the case of an open inverted V-flame responding to a fuel mass fraction oscillation imposed at the inlet.

Given that the empirical approach neglects crucial acoustic, hydrodynamic and thermal-diffusional processes, and DNS on the other hand cannot yet be routinely performed, we shall derive, from the reactive Navier-Stokes equations, an AEA theory for premixed combustion in the presence of enthalpy fluctuations, with a view to provide a mathematical framework in which the impact of enthalpy fluctuations on the flame dynamics and flame-acoustic coupling can be studied on the basis of first principles. In Part I of this study, we highlight the derivation and the main features of the results. In Part II, the general formulation will be applied to several special cases.

2. Formulation

2.1. *Governing equations and scalings*

Consider the combustion of a homogeneous premixed combustible mixture in a duct of width h^* and length $l^* \gg h^*$. The fresh mixture enters the duct at a constant mean velocity U_-^*. For simplicity, a one-step irreversible exothermic chemical reaction is assumed. The gaseous mixture consists of a single deficient reactant and an abundant component, and is assumed to obey the state equation for a perfect gas. The fresh mixture has a mean density $\rho_{-\infty}$ and temperature $\Theta_{-\infty}$, but small temperature and/or mass fraction fluctuations, which may be characterized as enthalpy disturbances, are assumed to be present in the oncoming flow.

Due to steady heat release, the mean temperature (density) behind the flame increases (decreases) to Θ_∞ (ρ_∞). A key non-dimensional parameter is the Zeldovich number,

$$\beta = E(\Theta_\infty - \Theta_{-\infty})/\mathcal{R}\Theta_\infty^2, \tag{2.1}$$

where E is the dimensional activation energy and $\mathcal{R}$ the universal gas constant. The flame propagates into the fresh mixture at a mean speed U_L, and has an intrinsic thickness $d = D_{th}^*/U_L$, where D_{th}^* is the thermal diffusivity. For later reference, we define the length ratio δ and the Mach number M,

$$\delta = d/h^*, \quad M = U_L/a^*,$$

where $a^* = (\gamma p_{-\infty}/\rho_{-\infty})^{\frac{1}{2}}$ is the speed of sound, with γ denoting the ratio of specific heats. Other relevant parameters are: the Prandtl number Pr, Lewis number Le, and the normalized gravity force $G = gh^*/U_L^2$.

Let (x, y, z) and t be space and time variables normalized by h^* and h^*/U_L respectively. The velocity $\mathbf{u} \equiv (u, v, w)$, density ρ, and temperature θ are non-dimensionalized by U_L, $\rho_{-\infty}$ and $\Theta_{-\infty}$, respectively. The non-dimensional pressure p is introduced by writing the dimensional pressure as $(p_{-\infty} + \rho_{-\infty} U_L^2 p)$. The velocity, pressure, temperature and fuel mass fraction Y satisfy the non-dimensional Navier-Stokes (N-S) equations for reactive flows with the reaction rate Ω being described by the Arrhenius law,

$$\Omega = \rho Y \exp\Big\{\beta(\frac{1}{\Theta_+} - \frac{1}{\theta})\Big\}, \tag{2.2}$$

where $\Theta_+ = 1 + q$ is the adiabatic flame temperature. On the assumption that the Zeldovich number is large, i.e., $\beta \gg 1$, the chemical reaction then occurs in a thin region of width $O(d/\beta)$ centered at the flame front. Assume that the flame front is given by $x = f(y, z, t)$. It is convenient to introduce a coordinate system attached to the front,

$$\xi = x - f(y, z, t), \quad \eta = y, \quad \zeta = z,$$

and to split the velocity $\mathbf{u}$ as $\mathbf{u} = u\,\mathbf{i} + \mathbf{v}$, where $\mathbf{i}$ is the unit vector along the duct. On assuming that the shear viscosity is independent of temperature and bulk viscosity is zero, the N-S equations can be written as

$$\frac{\partial \rho}{\partial t} + \frac{\partial m}{\partial \xi} + \bigtriangledown \cdot (\rho\, \mathbf{v}) = 0, \tag{2.3}$$

$$\rho \frac{\partial u}{\partial t} + m \frac{\partial u}{\partial \xi} + \rho\, \mathbf{v} \cdot \bigtriangledown u = -\frac{\partial p}{\partial \xi} + \delta \mathrm{Pr} \Big\{ \triangle u + \frac{1}{3} \frac{\partial}{\partial \xi} \Big(\frac{\partial s}{\partial \xi} + \bigtriangledown \cdot \mathbf{v} \Big) \Big\} - \rho G, \tag{2.4}$$

$$\rho \frac{\partial\, \mathbf{v}}{\partial t} + m \frac{\partial\, \mathbf{v}}{\partial \xi} + \rho\, \mathbf{v} \cdot \bigtriangledown \mathbf{v} = -\bigtriangledown p + \bigtriangledown f \frac{\partial p}{\partial \xi} + \delta \mathrm{Pr} \Big\{ \triangle \mathbf{v} + \frac{1}{3} \Big(\bigtriangledown - \bigtriangledown f \frac{\partial}{\partial \xi} \Big) \Big(\frac{\partial s}{\partial \xi} + \bigtriangledown \cdot \mathbf{v} \Big) \Big\}, \tag{2.5}$$

$$\rho \frac{\partial Y}{\partial t} + m \frac{\partial Y}{\partial \xi} + \rho\, \mathbf{v} \cdot \bigtriangledown Y = \delta \mathrm{Le}^{-1} \triangle Y - \delta\, \Omega, \tag{2.6}$$

$$\rho \frac{\partial \theta}{\partial t} + m \frac{\partial \theta}{\partial \xi} + \rho\, \mathbf{v} \cdot \bigtriangledown \theta = \delta \triangle \theta + \delta q\, \Omega + (\gamma - 1) M^2 \Big\{ \frac{\partial p}{\partial t} + m \frac{\partial p}{\partial \xi} + \rho\, \mathbf{v} \cdot \bigtriangledown p \Big\}, \tag{2.7}$$

$$1 + \gamma M^2 p = \rho\, \theta, \tag{2.8}$$

where $m = \rho s$,

$$s = u - f_t - \mathbf{v} \cdot \bigtriangledown f, \tag{2.9}$$

$$\triangle = \Big[1 + (\bigtriangledown f)^2\Big] \frac{\partial^2}{\partial \xi^2} + \bigtriangledown^2 - \bigtriangledown^2 f \frac{\partial}{\partial \xi} - 2 \frac{\partial}{\partial \xi} (\bigtriangledown f \cdot \bigtriangledown); \tag{2.10}$$

here operators $\bigtriangledown$ and $\bigtriangledown^2$ are defined with respect to the transverse variables η and ζ.

The AEA approach requires the Lewis number Le to be close to unity, or more precisely

$$\mathrm{Le} = 1 + \beta^{-1} l \quad \text{with} \quad l = O(1). \tag{2.11}$$

Instead of the reactant concentration Y, it is more convenient to work with a rescaled enthalpy h, defined via the relation $\theta + qY = 1 + q + \beta^{-1} h$. Then h satisfies

$$\rho \frac{\partial h}{\partial t} + m \frac{\partial h}{\partial \xi} + \rho\, \mathbf{v} \cdot \bigtriangledown h - \delta \triangle h = \delta l \triangle \theta + \beta (\gamma - 1) M^2 \Big\{ \frac{\partial p}{\partial t} + m \frac{\partial p}{\partial \xi} + \rho\, \mathbf{v} \cdot \bigtriangledown p \Big\}. \tag{2.12}$$

As in MM and WWMP, the hydrodynamic motion is assumed to occur on the length scale h^*. The corrugated flamelet regime then corresponds to

$$\delta = d/h^* \ll 1, \quad M \ll 1. \tag{2.13}$$

The whole flowfield is then described by four distinct asymptotic regions as is illustrated in Fig. 1 of WWMP. In addition to the thin $O(d/\beta)$ reaction and $O(d)$ preheat zones, there are also hydrodynamic and acoustic regions, which scale on h^* and $\lambda^* = O(h^*/M)$ respectively. The four regions are fully interactive in the sense that they all have to be considered in order to obtain the final complete solution.

The mathematical problem for enthalpy disturbances interacting with a flame turns out to be more complex than that for vortical and acoustic disturbances. The latter affect, to leading order, only the hydrodynamic region so that theories describing their impact on the flame and flame-acoustic coupling (e.g., WWMP and Wu & Law 2008) can be developed by using the results of MM. In contrast, enthalpy fluctuations penetrate into the preheat zone to reach the reaction sheet, thereby disturbing the chemical reaction and heat release. The results of MM, which were obtained without considering enthalpy fluctuations, are therefore not applicable, and the preheat zone has to be analyzed in detail in order to derive relevant jump conditions to be imposed on the flow motion in the outer hydrodynamic region.

2.2. *Preheat zone*

As implied above, the variable describing the preheat zone can be defined as

$$\widehat{\xi} = \xi/\delta. \tag{2.14}$$

The solution in this region expands as

$$\left.\begin{aligned} (\theta,\, h,\, m) &= \quad (\widehat{\theta}_0,\, \widehat{h}_0,\, m_0) + \delta(\widehat{\theta}_1,\, \widehat{h}_1,\, m_1) + \ldots, \\ (u,\, \mathbf{v},\, p) &= \quad (\widehat{u}_0,\, \widehat{\mathbf{v}}_0,\, \widehat{p}_0) + \delta(\widehat{u}_1,\, \widehat{\mathbf{v}}_1,\, \widehat{p}_1) + \ldots. \end{aligned}\right\}$$

On the length scale of d, the reaction zone appears as a sheet at $\widehat{\xi} = 0$. The analysis of its internal structure gives rise to the jump conditions (Matkowsky & Sivashinsky 1979)

$$\left.\begin{aligned} &[h] = [\theta] = 0, \quad \left[l\frac{\partial\theta}{\partial\widehat{\xi}} + \frac{\partial h}{\partial\widehat{\xi}}\right] = 0, \quad \left[1 + (\bigtriangledown f)^2\right]^{1/2}\left[\frac{\partial\theta}{\partial\widehat{\xi}}\right] = -q\exp\{\tfrac{1}{2}h(0)\}, \\ &[u] = [\mathbf{v}] = 0, \quad \left[\frac{\partial\,\mathbf{v}}{\partial\widehat{\xi}} + \frac{\partial u}{\partial\widehat{\xi}}\bigtriangledown f\right] = 0, \quad [p] = \frac{4}{3}\mathrm{Pr}\Big(1 + (\bigtriangledown f)^2\Big)\left[\frac{\partial u}{\partial\widehat{\xi}}\right], \end{aligned}\right\} \tag{2.15}$$

which relate the flow quantities on the two sides of the sheet.

The leading-order temperature and enthalpy, $\widehat{\theta}_0$ and $\widehat{h}_0$, are governed by equations

$$m_0\frac{\partial\widehat{\theta}_0}{\partial\widehat{\xi}} - \kappa\frac{\partial^2\widehat{\theta}_0}{\partial\widehat{\xi}^2} = 0, \qquad m_0\frac{\partial\widehat{h}_0}{\partial\widehat{\xi}} - \kappa\frac{\partial^2\widehat{h}_0}{\partial\widehat{\xi}^2} = l\kappa\frac{\partial^2\widehat{\theta}_0}{\partial\widehat{\xi}^2}, \tag{2.16}$$

where we have put $\kappa(\eta,\zeta,t) = 1 + (\bigtriangledown f_0)^2$. The solution satisfying the above conditions is found to be

$$\widehat{\theta}_0 = \begin{cases} 1 + q\exp\{\dfrac{m_0}{\kappa}\widehat{\xi}\} & \widehat{\xi} < 0, \\ 1 + q & \widehat{\xi} > 0, \end{cases} \tag{2.17}$$

$$\widehat{h}_0 = \begin{cases} h_{-\infty} - \dfrac{qlm_0}{\kappa}\widehat{\xi}\exp\{\dfrac{m_0}{\kappa}\widehat{\xi}\} & \widehat{\xi} < 0, \\ h_{-\infty} & \widehat{\xi} > 0, \end{cases} \tag{2.18}$$

where $m_0 = \left[1 + (\triangledown f_0)^2\right]^{\frac{1}{2}} \exp\{\frac{1}{2}h_{-\infty}\}$. Function $h_{-\infty}(\eta, \zeta, t)$ represents the enthalpy approaching the flame, and matches with the solution in the hydrodynamic zone. In the classical work of MM and Pelce & Clavin (1982), $h_{-\infty} = 0$ on the assumption that no enthalpy fluctuations are present in the oncoming mixture.

Next we consider the velocity, which satisfies

$$m_0\frac{\partial \widehat{u}_0}{\partial \widehat{\xi}} - \Pr\Big\{\kappa\frac{\partial^2 \widehat{u}_0}{\partial \widehat{\xi}^2} + \frac{1}{3}\frac{\partial^2 \widehat{s}_0}{\partial \widehat{\xi}^2}\Big\} = -\frac{\partial \widehat{p}_0}{\partial \widehat{\xi}}, \tag{2.19}$$

$$m_0\frac{\partial \widehat{\mathbf{v}}_0}{\partial \widehat{\xi}} - \Pr\Big\{\kappa\frac{\partial^2 \widehat{\mathbf{v}}_0}{\partial \widehat{\xi}^2} - \frac{1}{3}\frac{\partial^2 \widehat{s}_0}{\partial \widehat{\xi}^2}\triangledown f_0\Big\} = -\triangledown \widehat{p}_0 + \frac{\partial \widehat{p}_0}{\partial \widehat{\xi}}\triangledown f_0. \tag{2.20}$$

The solution is found to be

$$\widehat{u}_0 = \begin{cases} u_0^- + \dfrac{qm_0}{\kappa}\exp\{\dfrac{m_0}{\kappa}\widehat{\xi}\} & \widehat{\xi} < 0, \\ u_0^- + \dfrac{qm_0}{\kappa} & \widehat{\xi} > 0, \end{cases} \tag{2.21}$$

$$\widehat{\mathbf{v}}_0 = \begin{cases} \mathbf{v}_0^- - \dfrac{qm_0}{\kappa}\exp\{\dfrac{m_0}{\kappa}\widehat{\xi}\}\triangledown f_0 & \widehat{\xi} < 0, \\ \mathbf{v}_0^- - \dfrac{qm_0}{\kappa}\triangledown f_0, & \widehat{\xi} > 0, \end{cases} \tag{2.22}$$

$$\widehat{p}_0 = \begin{cases} p_0^- + (\frac{4}{3}Pr - 1)\dfrac{qm_0^2}{\kappa}\exp\{\dfrac{m_0}{\kappa}\widehat{\xi}\} & \widehat{\xi} < 0, \\ p_0^- - \dfrac{qm_0^2}{\kappa} & \widehat{\xi} > 0, \end{cases} \tag{2.23}$$

where by matching with the hydrodynamic solution, the integration constants u_0^-, $\mathbf{v}_0^-$ and p_0^- are found to be the velocity and pressure of the flow at the unburned side of the flame. Taking the limit $\widehat{\xi} \to -\infty$ in Eq.(2.9) yields the leading-order front equation

$$\frac{\partial f_0}{\partial t} = u_0^- - \mathbf{v}_0^- \cdot \triangledown f_0 - \left[1 + (\triangledown f_0)^2\right]^{\frac{1}{2}} \exp\{\tfrac{1}{2}h_{-\infty}\}. \tag{2.24}$$

The analysis can be carried to the next order. The continuity equation at this order reads

$$\frac{\partial m_1}{\partial \widehat{\xi}} = -\frac{\partial \widehat{\rho}_0}{\partial t} + \triangledown \cdot (\widehat{\rho}_0 \widehat{\mathbf{v}}_0),$$

and it can be integrated to give

$$m_1 = \begin{cases} M + \Gamma\ln(1+q\,\mathrm{e}^{m_0\widehat{\xi}/\kappa}) - \widehat{\xi}\,\triangledown\cdot\mathbf{v}_0^- - \dfrac{m_0}{\kappa}\dfrac{\tilde{D}}{\tilde{D}t}\left(\dfrac{\kappa}{m_0}\right)\dfrac{q\widehat{\xi}\,\mathrm{e}^{m_0\widehat{\xi}/\kappa}}{1+q\,\mathrm{e}^{m_0\widehat{\xi}/\kappa}} & \widehat{\xi} < 0, \\ M + \Gamma\ln(1+q) - \dfrac{\widehat{\xi}}{1+q}\left\{\triangledown\cdot\mathbf{v}_0^- - q\,\triangledown\cdot(\dfrac{m_0}{\kappa}\triangledown f_0)\right\} & \widehat{\xi} > 0, \end{cases}$$

where $M(\eta,\zeta,t)$ is a function to be found, and

$$\Gamma(\eta,\zeta,t)=\frac{D}{Dt}(\frac{\kappa}{m_0})+\frac{\kappa}{m_0}\,\triangledown\cdot\mathbf{v}_0^-+\triangledown^2 f_0,$$

$$\frac{D}{Dt}=\frac{\partial}{\partial t}+\mathbf{v}_0^-\cdot\triangledown,\qquad \frac{\tilde{D}}{\tilde{D}t}=\frac{D}{Dt}+\frac{m_0}{\kappa}(\triangledown f_0\cdot\triangledown).$$

The equations governing the transport of $\widehat{\theta}_1$ and $\widehat{h}_1$ are

$$m_0\frac{\partial\widehat{\theta}_1}{\partial\widehat{\xi}}-\kappa\frac{\partial^2\widehat{\theta}_1}{\partial\widehat{\xi}^2}=-m_1\frac{\partial\widehat{\theta}_0}{\partial\widehat{\xi}}+2\triangledown f_0\cdot\triangledown f_1\frac{\partial^2\widehat{\theta}_0}{\partial\widehat{\xi}^2}-\widehat{\rho}_0(\frac{\partial\widehat{\theta}_0}{\partial t}+\widehat{\mathbf{v}}_0\cdot\triangledown\widehat{\theta}_0)-\frac{\partial}{\partial\widehat{\xi}}(\widehat{\theta}_0\triangledown^2 f_0+2\triangledown f_0\cdot\triangledown\widehat{\theta}_0), \tag{2.25}$$

$$\begin{aligned}m_0\frac{\partial\widehat{h}_1}{\partial\widehat{\xi}}-\kappa\frac{\partial^2\widehat{h}_1}{\partial\widehat{\xi}^2}=l\kappa\frac{\partial^2\widehat{\theta}_1}{\partial\widehat{\xi}^2}-m_1\frac{\partial\widehat{h}_0}{\partial\widehat{\xi}}+2\,\triangledown f_0\cdot\triangledown f_1\frac{\partial^2}{\partial\widehat{\xi}^2}(\widehat{h}_0+l\widehat{\theta}_0)-\widehat{\rho}_0(\frac{\partial\widehat{h}_0}{\partial t}+\widehat{\mathbf{v}}_0\cdot\triangledown\widehat{h}_0)\\ -\frac{\partial}{\partial\widehat{\xi}}\Big\{(\widehat{h}_0+l\widehat{\theta}_0)\,\triangledown^2 f_0+2\,\triangledown f_0\cdot\triangledown(\widehat{h}_0+l\widehat{\theta}_0)\Big\}.\end{aligned} \tag{2.26}$$

Expansion of the jumps across the reaction zone, Eq.(2.15), gives the relations

$$\left.\begin{aligned}[\widehat{h}_1]=[\widehat{\theta}_1]=0,\quad \left[\frac{\partial\widehat{h}_1}{\partial\widehat{\xi}}\right]=-l\left[\frac{\partial\widehat{\theta}_1}{\partial\widehat{\xi}}\right],\\ \kappa\left[\frac{\partial\widehat{\theta}_1}{\partial\widehat{\xi}}\right]=-\tfrac{1}{2}qm_0\widehat{h}_1(0)+\frac{qm_0}{\kappa}\,\triangledown f_0\cdot\triangledown f_1,\\ [\widehat{p}_1]=\tfrac{4}{3}\mathrm{Pr}\left[\frac{\partial\widehat{s}_1}{\partial\widehat{\xi}}\right]=\tfrac{4}{3}\mathrm{Pr}\left\{\kappa\left[\frac{\partial\widehat{u}_1}{\partial\widehat{\xi}}\right]+2\,\triangledown f_0\cdot\triangledown f_1\left[\frac{\partial\widehat{u}_0}{\partial\widehat{\xi}}\right]\right\}.\end{aligned}\right\} \tag{2.27}$$

Noting first that $\widehat{\theta}_1=0$ for $\widehat{\xi}>0$, and then integrating Eq.(2.25) with respect to $\widehat{\xi}$ from $-\infty$ to 0, we obtain

$$\left(\frac{\partial\widehat{\theta}_1}{\partial\widehat{\xi}}\right)_{\widehat{\xi}=0^-}=\frac{q}{\kappa}M+\frac{1+q}{\kappa}\ln(1+q)\Gamma-\frac{2qm_0}{\kappa^2}\,\triangledown f_0\cdot\triangledown f_1. \tag{2.28}$$

Integrating Eq.(2.26) and matching with the solution in the hydrodynamic region, we have

$$\left(m_0\widehat{h}_1-\kappa\frac{\partial\widehat{h}_1}{\partial\widehat{\xi}}\right)_{\widehat{\xi}=0^-}=l\kappa\left(\frac{\partial\widehat{\theta}_1}{\partial\widehat{\xi}}\right)_{\widehat{\xi}=0^-}-l\mathcal{D}\Gamma+m_0h_1^--\kappa\frac{\partial h_0^-}{\partial\xi}+\ln(1+q)\frac{\kappa}{m_0}\frac{\tilde{D}}{\tilde{D}t}h_{-\infty}, \tag{2.29}$$

where

$$\mathcal{D}(q)=\int_0^\infty \ln(1+q\,\mathrm{e}^{-x})\,\mathrm{d}\,x.$$

For $\widehat{\xi}>0$,

$$\widehat{h}_1=\widehat{h}_1(0)-\frac{1}{(1+q)m_0}\left\{\frac{Dh_{-\infty}}{Dt}-\frac{qm_0}{\kappa}\,\triangledown f_0\cdot\triangledown h_{-\infty}\right\}\widehat{\xi}\equiv\widehat{h}_1(0)+\frac{\partial h_0^+}{\partial\xi}\xi. \tag{2.30}$$

As will be shown later, the term proportional to $\widehat{\xi}$ matches with the hydrodynamic solution automatically, while matching the constant term yields

$$\widehat{h}_1(0) = h_1^+ = h_1^- + [[h_1]]. \tag{2.31}$$

Inserting Eq.(2.30) into Eq.(2.27) gives

$$-\left(\frac{\partial \widehat{h}_1}{\partial \widehat{\xi}}\right)_{\widehat{\xi}=0^-} = -\frac{\partial h_0^+}{\partial \xi} + l\left(\frac{\partial \widehat{\theta}_1}{\partial \widehat{\xi}}\right)_{\widehat{\xi}=0^-}. \tag{2.32}$$

It follows from Eq.(2.29) and Eq.(2.32) that

$$[[h_1]] = \left(\ln(1+q) + \frac{q}{1+q}\right)\frac{\kappa}{m_0^2}\frac{\tilde{D}}{\tilde{D}t}h_{-\infty} - \frac{l\mathcal{D}}{m_0}\Gamma, \tag{2.33}$$

where we have used the result $\left[\left[\frac{\partial h_0}{\partial \xi}\right]\right] = \frac{q}{(1+q)m_0}\frac{\tilde{D}}{\tilde{D}t}h_{-\infty}$, which is to be derived later; see Eq.(2.48). Substituting Eq.(2.28) and Eq.(2.31) together with Eq.(2.33) into Eq.(2.27), we find

$$M = -\mathrm{M}_a\Gamma + \frac{m_0}{\kappa}\bigtriangledown f_0\cdot\bigtriangledown f_1 + \tfrac{1}{2}\left\{\frac{\kappa}{m_0}\left(\ln(1+q) + \frac{q}{1+q}\right)\frac{\tilde{D}}{\tilde{D}t}h_{-\infty} + m_0h_1^-\right\}, \tag{2.34}$$

$$\mathrm{M}_a = \left(\frac{1+q}{q}\ln(1+q) + \tfrac{1}{2}l\mathcal{D}\right).$$

As in MM, the equations for u_1 and $\mathbf{v}_1$ are combined to give

$$\begin{aligned}
&m_0\frac{\partial}{\partial\widehat{\xi}}(\widehat{\mathbf{v}}_1 + \widehat{u}_1\bigtriangledown f_0) - Pr\kappa\frac{\partial^2}{\partial\widehat{\xi}^2}(\widehat{\mathbf{v}}_1 + \widehat{u}_1\bigtriangledown f_0)\\
&= -\widehat{\rho}_0(\frac{\partial}{\partial t} + \widehat{\mathbf{v}}_0\cdot\bigtriangledown)(\widehat{\mathbf{v}}_0 + \widehat{u}_0\bigtriangledown f_0) + \widehat{\rho}_0\widehat{u}_0(\frac{\partial}{\partial t} + \widehat{\mathbf{v}}_0\cdot\bigtriangledown)\bigtriangledown f_0\\
&\quad+\mathrm{Pr}(\bigtriangledown\kappa)\frac{\partial\widehat{u}_0}{\partial\widehat{\xi}} + \left(\bigtriangledown f_1\frac{\partial}{\partial\widehat{\xi}} - \bigtriangledown\right)(\widehat{p}_0 - \frac{Pr}{3}\frac{\partial\widehat{s}_0}{\partial\widehat{\xi}}) - \widehat{\rho}_0G\bigtriangledown f_0.
\end{aligned} \tag{2.35}$$

After inserting Eqs.(2.21)–(2.23) into the right-hand side, the equation can be integrated with respect to $\widehat{\xi}$. Matching with the hydrodynamic solution shows that

$$\begin{aligned}
[[\mathbf{v}_1 + u_1\bigtriangledown f_0]] = \mathrm{Pr}\frac{\kappa}{m_0}&\left[\left[\frac{\partial}{\partial\xi}(\mathbf{v}_0 + u_0\bigtriangledown f_0)\right]\right]\\
&+\frac{\kappa}{m_0^2}\ln(1+q)\left\{\frac{\tilde{D}\,\mathbf{v}_0^-}{\tilde{D}t} + \bigtriangledown f_0\frac{\tilde{D}u_0^-}{\tilde{D}t} + \frac{m_0}{\kappa}\frac{\tilde{D}}{\tilde{D}t}\bigtriangledown f_0 + G\bigtriangledown f_0\right\}\\
&-\frac{qm_0}{\kappa}\bigtriangledown f_1 - \frac{q}{\kappa}(\bigtriangledown f_0\cdot\bigtriangledown)\bigtriangledown f_0 + \mathrm{Pr}\frac{q}{\kappa}\bigtriangledown\kappa - (\mathrm{Pr}-1)\frac{q}{m_0}\bigtriangledown m_0.
\end{aligned} \tag{2.36}$$

Expansion of $m = \rho s$ and the state equation yields $\widehat{s}_1 = m_1\widehat{\theta}_0 + m_0\widehat{\theta}_1$, while expansion of Eq.(2.9) gives

$$\kappa\widehat{u}_1 = \widehat{s}_1 + \frac{\partial f_1}{\partial t} + \widehat{\mathbf{v}}_0\cdot\bigtriangledown f_1 + (\widehat{\mathbf{v}}_1 + \widehat{u}_1\bigtriangledown f_0)\cdot\bigtriangledown f_0. \tag{2.37}$$

Now taking the limits $\widehat{\xi}\to\pm\infty$ in Eq.(2.37) and matching u_1 with the hydrodynamic solution, we find that

$$[[u_1]] = -\frac{lq\mathcal{D}}{2\kappa}\Gamma + \chi\left\{\frac{\kappa}{m_0}\left[\left[\frac{\partial u_0}{\partial \xi}\right]\right] - \frac{q}{\kappa}\bigtriangledown^2 f_0 + \frac{2qm_0}{\kappa^2}\bigtriangledown f_0\cdot\bigtriangledown(\frac{\kappa}{m_0})\right\}$$
$$-\frac{qm_0}{\kappa^2}\bigtriangledown f_0\cdot\bigtriangledown f_1 + \frac{q}{2\kappa}\left(1-\frac{1+q}{q}\ln(1+q)\right)\bigtriangledown f_0\cdot\bigtriangledown h_{-\infty}$$
$$+\frac{q}{2\kappa}\left\{\frac{\kappa}{m_0}\left(\frac{q}{1+q}+\ln(1+q)\right)\frac{\tilde{D}}{\tilde{D}t}h_{-\infty} + m_0 h_1^-\right\}, \tag{2.38}$$

$$\frac{\partial f_1}{\partial t} + \mathbf{v}_0^-\cdot\bigtriangledown f_1 + \mathbf{v}_1^-\cdot\bigtriangledown f_0 = u_1^- - \frac{m_0}{\kappa}\bigtriangledown f_0\cdot\bigtriangledown f_1 + \mathrm{M}_a\Gamma$$
$$-\tfrac{1}{2}\left\{\frac{\kappa}{m_0}\left(\ln(1+q)+\frac{q}{1+q}\right)\frac{\tilde{D}}{\tilde{D}t}h_{-\infty} + m_0 h_1^-\right\}, \tag{2.39}$$

where we have put $\chi = Pr + \frac{1+q}{q}\ln(1+q)$.

The jump in the pressure can be found from the longitudinal momentum equation

$$\frac{\partial \widehat{p}_1}{\partial \widehat{\xi}} = -m_0\frac{\partial \widehat{u}_1}{\partial \widehat{\xi}} - m_1\frac{\partial \widehat{u}_0}{\partial \widehat{\xi}} - \widehat{\rho}_0(\frac{\partial \widehat{u}_0}{\partial t} + \widehat{\mathbf{v}}_0\cdot\bigtriangledown \widehat{u}_0) - \widehat{\rho}_0 G$$
$$+\mathrm{Pr}\frac{\partial}{\partial \widehat{\xi}}\left\{\kappa\frac{\partial \widehat{u}_1}{\partial \widehat{\xi}} + 2\bigtriangledown f_0\cdot\bigtriangledown f_1\frac{\partial \widehat{u}_0}{\partial \widehat{\xi}} - \widehat{u}_0\bigtriangledown^2 f_0 - 2\bigtriangledown f_0\cdot\bigtriangledown \widehat{u}_0 + \frac{1}{3}(\frac{\partial \widehat{s}_1}{\partial \widehat{\xi}} + \bigtriangledown\cdot\widehat{\mathbf{v}}_0)\right\}.$$

Integrating with respect to $\widehat{\xi}$, and matching $\widehat{p}_1$ with its counterpart in the hydrodynamic zone, we obtain

$$[[p_1]] = -2m_0[[u_1]] + (Pr+\chi)\left\{\kappa\left[\left[\frac{\partial u_0}{\partial \xi}\right]\right] - \frac{qm_0}{\kappa}\bigtriangledown^2 f_0 + \frac{2qm_0^2}{\kappa^2}\bigtriangledown f_0\cdot\bigtriangledown(\frac{\kappa}{m_0})\right\}$$
$$+\frac{qm_0}{\kappa}\bigtriangledown^2 f_0 - \frac{qm_0^2}{\kappa^2}\left(2\bigtriangledown f_0\cdot\bigtriangledown f_1 + \bigtriangledown f_0\cdot\bigtriangledown(\frac{\kappa}{m_0})\right)$$
$$+\left\{\frac{\kappa}{m_0}\frac{\tilde{D}u_0^-}{\tilde{D}t} + \frac{m_0}{\kappa}\frac{\tilde{D}}{\tilde{D}t}(\frac{\kappa}{m_0}) + G\Big(\frac{\kappa}{m_0}\Big)\right\}\ln(1+q)$$
$$+\frac{qm_0}{2\kappa}\left(1-\frac{1+q}{q}\ln(1+q)\right)\bigtriangledown f_0\cdot\bigtriangledown h_{-\infty}. \tag{2.40}$$

2.3. *Hydrodynamic zone*

In the hydrodynamic zone, the mean density $R = R_- = 1$ for $\xi < 0$ and $R = R_+ = 1/(1+q)$ for $\xi > 0$. The solution for the flowfield, flame interface and enthalpy, expands as

$$(u,\, \mathbf{v},\, p,\, f,\, h) = (u_0,\, \mathbf{v}_0,\, p_0,\, f_0, h_0) + \delta(u_1,\, \mathbf{v}_1,\, f_1, h_1) + \ldots. \tag{2.41}$$

The expansion should also consist of $O(\beta M)$ terms because the acoustic pressure induces an $O(\beta M)$ enthalpy fluctuation, which in turn contributes an $O(\beta M)$ correction to the flame speed (WWMP). In order to avoid complicating further an already complex analysis, this effect is neglected here.

Substitution of Eq.(2.41) into Eqs.(2.3)–(2.5) leads to the equations governing $(u_0,\, \mathbf{v}_0,\, p_0)$:

$$\left.\begin{aligned} \frac{\partial s_0}{\partial \xi} + \bigtriangledown \cdot \mathbf{v}_0 = &\quad 0, \\ R\left\{\frac{\partial u_0}{\partial t} + s_0\frac{\partial u_0}{\partial \xi} + \mathbf{v}_0 \cdot \bigtriangledown u_0\right\} = &\quad -\frac{\partial p_0}{\partial \xi} - RG, \\ R\left\{\frac{\partial \mathbf{v}_0}{\partial t} + s_0\frac{\partial \mathbf{v}_0}{\partial \xi} + \mathbf{v}_0 \cdot \bigtriangledown \mathbf{v}_0\right\} = &\quad -\bigtriangledown p_0 + \bigtriangledown f_0\frac{\partial p_0}{\partial \xi}, \end{aligned}\right\} \tag{2.42}$$

where $s_0 = u_0 - f_{0,t} - \mathbf{v}_0 \cdot \bigtriangledown f_0$. It follows from Eq.(2.18) and Eqs.(2.21)–(2.23) that across the preheat zone, $[[h_0]] = 0$ and

$$[[u_0]] = \frac{qm_0}{\kappa}, \quad [[\mathbf{v}_0]] = -\frac{qm}{\kappa}\bigtriangledown f_0, \quad [[p_0]] = -q\exp\{h_{-\infty}\}, \tag{2.43}$$

where $h_{-\infty} = h_0(0,\eta,\zeta,t)$.

The momentum equations for u_0 and $\mathbf{v}_0$ can be combined to give

$$m_0\frac{\partial}{\partial \xi}(\mathbf{v}_0 + u_0 \bigtriangledown f_0) + R\bigtriangledown f_0(\frac{\partial}{\partial t} + \mathbf{v}_0 \cdot\bigtriangledown)u_0 + R(\frac{\partial}{\partial t} + \mathbf{v}_0 \cdot\bigtriangledown)\,\mathbf{v}_0 = -\bigtriangledown p_0 - RG\bigtriangledown f_0.$$

Taking the limits $\xi \to 0^{\pm}$, and subtracting the results, we obtain

$$\left[\left[\frac{\partial}{\partial \xi}(\mathbf{v}_0 + u_0 \bigtriangledown f_0)\right]\right] = \frac{q}{(1+q)m_0}\left\{\frac{\tilde{D}\,\mathbf{v}_0^-}{\tilde{D}t} + \bigtriangledown f_0\frac{\tilde{D}u_0^-}{\tilde{D}t} + \frac{m_0}{\kappa}\frac{\tilde{D}}{\tilde{D}t}\bigtriangledown f_0 + G\bigtriangledown f_0\right\}$$
$$-\frac{qm_0}{\kappa^2}(\bigtriangledown f_0 \cdot \bigtriangledown)\bigtriangledown f_0 + \frac{q}{m_0}\bigtriangledown(\frac{m_0^2}{\kappa}). \tag{2.44}$$

The continuity equation implies that $\left[\left[\frac{\partial u_0}{\partial \xi} - \frac{\partial\,\mathbf{v}_0}{\partial \xi}\cdot\bigtriangledown f_0\right]\right] = -q\bigtriangledown\cdot\left(\frac{m_0}{\kappa}\bigtriangledown f_0\right)$, which may be rewritten as

$$\left[\left[\frac{\partial u_0}{\partial \xi}\right]\right] = \frac{\bigtriangledown f_0}{\kappa}\cdot\left[\left[\frac{\partial}{\partial \xi}(\mathbf{v}_0 + u_0 \bigtriangledown f_0)\right]\right] + \frac{q}{\kappa}\bigtriangledown\cdot\left(\frac{m_0}{\kappa}\bigtriangledown f_0\right). \tag{2.45}$$

To determine $h_{-\infty}$, we need to solve the equation governing the transport of the enthalpy fluctuation

$$\frac{\partial h_0}{\partial t} + s_0\frac{\partial h_0}{\partial \xi} + \mathbf{v}_0 \cdot \bigtriangledown h_0 = 0. \tag{2.46}$$

It follows that

$$h_0 \to h_{-\infty} + \frac{\partial h_0^{\pm}}{\partial \xi}\xi, \quad \text{as} \quad \xi \to 0^{\pm}, \tag{2.47}$$

where

$$\frac{\partial h_0^-}{\partial \xi} = -\frac{1}{m_0}\frac{Dh_{-\infty}}{Dt}, \quad \frac{\partial h_0^+}{\partial \xi} = -\frac{1}{(1+q)m_0}\left\{\frac{Dh_{-\infty}}{Dt} - \frac{qm_0}{\kappa}\bigtriangledown f_0 \cdot \bigtriangledown h_{-\infty}\right\}, \tag{2.48}$$

as can be obtained by taking the limits $\xi \to 0^{\pm}$ in Eq.(2.46).

The $O(\delta)$ flowfield, $(u_1, \mathbf{v}_1, p_1)$, satisfies a linearized version of Eq.(2.42) but consisting also of viscous terms (see MM). These equations will not be further considered, because in practice it is more convenient to construct a composite approximation by retaining the $O(\delta)$ viscous terms at leading-order, and imposing the jump conditions with $O(\delta)$ accuracy. The latter follow from combining Eq.(2.43) with Eq.(2.38) and Eq.(2.40). Note that $-(qm_0/\kappa^2)\,\triangledown f_0\cdot\triangledown f_1+qm_0h_1^-/(2\kappa)$ in Eq.(2.38) is simply the second term in the expansion of qm/κ for $f=f_0+\delta f_1+\ldots$ and $h_{-\infty}=h_{-\infty}+\delta h_1^-+\ldots$, and so it can be absorbed into qm/κ with the understanding that f and $h_{-\infty}$ now stand for the two-term approximations. Therefore, up to $O(\delta)$ accuracy,

$$[[u]]=\frac{qm}{\kappa}+\delta\Bigg\{-\frac{ql\mathcal{D}}{2\kappa}\Gamma+\frac{q\chi}{(1+q)m^2}\Big[\frac{\tilde{D}\,\mathbf{v}^-}{\tilde{D}t}+\triangledown f\frac{\tilde{D}u^-}{\tilde{D}t}+\frac{m}{\kappa}\frac{\tilde{D}}{\tilde{D}t}\triangledown f+G\,\triangledown f\Big]\cdot\triangledown f$$
$$+\frac{q}{2\kappa}\left[(\mathrm{Pr}{+}1)\,\triangledown f\cdot\triangledown h_{-\infty}+\frac{\kappa}{m}\Big[\frac{q}{1+q}+\ln(1{+}q)\Big]\frac{\tilde{D}h_{-\infty}}{\tilde{D}t}\right]\Bigg\}. \tag{2.49}$$

Similarly, the transverse velocity and pressure jumps are found to be

$$[[\mathbf{v}]]=-[[u]]\,\triangledown f+\delta\Big\{\frac{q\chi\kappa}{(1+q)m^2}\Big[\frac{\tilde{D}\,\mathbf{v}^-}{\tilde{D}t}+\triangledown f\frac{\tilde{D}u^-}{\tilde{D}t}+\frac{m}{\kappa}\frac{\tilde{D}}{\tilde{D}t}\triangledown f+G\,\triangledown f\Big]$$
$$+\tfrac{1}{2}(\mathrm{Pr}+1)q\,\triangledown h_{-\infty}\Big\}, \tag{2.50}$$

$$[[p]]=-q\exp\{h_{-\infty}\}-2m[[u]]+\delta\Big\{\frac{qm}{\kappa}\,\triangledown^2 f+\Big[\frac{\kappa}{m}\frac{\tilde{D}u^-}{\tilde{D}t}+\frac{m}{\kappa}\frac{\tilde{D}}{\tilde{D}t}(\frac{\kappa}{m})+G\frac{\kappa}{m}\Big]\ln(1{+}q)$$
$$-\frac{qm}{2\kappa^2}\,\triangledown f\cdot\triangledown\kappa+\frac{q(\mathrm{Pr}+\chi)}{(1+q)m}\Big[\frac{\tilde{D}\mathbf{v}^-}{\tilde{D}t}+\triangledown f\frac{\tilde{D}u^-}{\tilde{D}t}+\frac{m}{\kappa}\frac{\tilde{D}}{\tilde{D}t}\triangledown f+G\,\triangledown f\Big]\cdot\triangledown f$$
$$+\frac{qm}{\kappa}(\mathrm{Pr}+1)\,\triangledown f\cdot\triangledown h_{-\infty}\Big\}. \tag{2.51}$$

The equation governing the flame front is

$$f_t+\mathbf{v}^-\cdot\triangledown f=u^--m+\delta\Big\{\mathrm{M}_a\Gamma-\frac{\kappa}{2m}\Big[\ln(1{+}q)+\frac{q}{1+q}\Big]\frac{\tilde{D}h_{-\infty}}{\tilde{D}t}\Big\}. \tag{2.52}$$

3. Acoustic-flame-enthalpy interaction theory

The results obtained in the previous section, which generalize those of MM, allow us to show that an unsteady flame emits spontaneous sound waves, which act simultaneously on the flame. This two-way coupling is primarily facilitated by the hydrodynamic motion as in WWMP, but is now further modified by enthalpy fluctuations.

3.1. *Acoustic zone*

The variable describing the acoustic motion ambient to the hydrodynamic region is

$$\tilde{\xi}=M\xi. \tag{3.1}$$

The motion is a longitudinal oscillation about the uniform mean background, and the solution can be written as

$$\big(u,\rho,\theta\big)=\big(U_\pm,R_\pm,\Theta_\pm\big)+\Big(u_a(\tilde{\xi},t),M\rho_a(\tilde{\xi},t),M\theta_a(\tilde{\xi},t)\Big),\quad p=M^{-1}p_a(\tilde{\xi},t), \tag{3.2}$$

where $U_\pm$ are the mean velocities behind and in front of the flame, respectively. The unsteady field is governed by the linearized acoustic equations. Elimination of θ_a and ρ_a among those equations yields the wave equation for the pressure p_a and u_a,

$$R\frac{\partial^2 p_a}{\partial t^2}-\frac{\partial^2 p_a}{\partial\tilde{\xi}^2}=0,\quad\text{and}\quad R\frac{\partial u_a}{\partial t}=-\frac{\partial p_a}{\partial\tilde{\xi}}. \tag{3.3}$$

As $\tilde{\xi} \to \pm 0$,

$$u_a \to u_a(0^{\pm}, t) + \ldots, \quad p_a \to p_a(0, t) + p_{a,\tilde{\xi}}(0^{\pm}, t)\tilde{\xi} + \ldots .$$

As will be shown in Sec.3.2, the acoustic pressure is continuous across the flame, but the flame induces a jump in u_a, i.e.,

$$[p_a] = 0, \tag{3.4}$$

$$[u_a] = q\Big\{\overline{(1 + (\triangledown F)^2)^{\frac{1}{2}} \exp\{\tfrac{1}{2}h_{-\infty}\}} - 1\Big\} - \delta q\Big\{\frac{l\mathcal{D}}{2}\frac{\partial}{\partial t}\overline{(1 + (\triangledown F)^2)^{\frac{1}{2}} \exp\{-\tfrac{1}{2}h_{-\infty}\}}$$
$$+\Big(\frac{q}{1+q} + \ln(1+q)\Big)\overline{(1 + (\triangledown F)^2)^{\frac{1}{2}}\frac{\tilde{D}}{\tilde{D}t}\exp\{-\tfrac{1}{2}h_{-\infty}\}}\Big\}, \tag{3.5}$$

where $\overline{\phi}$ stands for the space average of ϕ in the (η, ζ) plane, and F is defined in Eq.(3.7) below. At leading order, Eq.(3.12) reduces to

$$[u_a] = q\Big\{\overline{(1 + (\triangledown F)^2)^{\frac{1}{2}} \exp\{\tfrac{1}{2}h_{-\infty}\}} - 1\Big\}. \tag{3.6}$$

Obviously, the jump $[u_a]$ acts as an acoustic source, which on the scale of acoustic wavelengths is equivalent to a concentrated unsteady heat release rate. The result indicates that (a) an unsteadily wrinkling flame is deemed to generate an acoustic field spontaneously, and (b) enthalpy fluctuations radiate sound waves even when the flame is planar. As will be shown in Sec.3.2, sound waves in turn exert a leading-order back effect on the flame and hydrodynamics. This is in contrast to typical aeroacoustic problems, where sound waves are merely a passive by-product.

3.2. *Hydrodynamic region*

In the hydrodynamic region, u_a and $p_{a,\xi}$ appear spatially uniform on either side of the flame, and can be approximated by their values at $\tilde{\xi} = 0^{\pm}$. In order to facilitate the matching with the solution in the acoustic region, we subtract from the total field the acoustic components as well as the mean background flow by writing

$$\left.\begin{aligned} u =& \quad U_{\pm} + u_a(0^{\pm}, t) + U, \quad f = F_a + F, \\ p =& \quad M^{-1}p_a(0, t) + P_{\pm} + p_{a,\tilde{\xi}}(0^{\pm}, t)(\xi + F) + P, \end{aligned}\right\} \tag{3.7}$$

where $P_{\pm}$ is the mean pressure (with $P_+ - P_- = -q$), and $F_a' = U_- - 1 + u_a(0^-, t)$. Let $\mathbf{v} = \mathbf{V}$. Then the hydrodynamic field, to $O(\delta)$ accuracy, satisfies the equations

$$\left.\begin{aligned} \frac{\partial U}{\partial \xi} + \triangledown \cdot \mathbf{V} =& \quad \frac{\partial \mathbf{V}}{\partial \xi} \cdot \triangledown F, \\ R\Big[\frac{\partial \tilde{U}}{\partial t} + S\frac{\partial U}{\partial \xi} + \mathbf{V} \cdot \triangledown U\Big] + \Big[1 + R\mathcal{J}h(\xi)\Big]\frac{\partial U}{\partial \xi} =& \quad -\frac{\partial P}{\partial \xi} + \delta \mathrm{Pr}\Delta U, \\ R\Big[\frac{\partial \mathbf{V}}{\partial t} + S\frac{\partial \mathbf{V}}{\partial \xi} + \mathbf{V} \cdot \triangledown \mathbf{V}\Big] + \Big[1 + R\mathcal{J}h(\xi)\Big]\frac{\partial \mathbf{V}}{\partial \xi} =& - \triangledown P + \triangledown F\frac{\partial P}{\partial \xi} + \delta \mathrm{Pr}\Delta \mathbf{V}, \end{aligned}\right\} \tag{3.8}$$

where $h(\xi)$ is the Heaviside step function, and $\mathcal{J} = [u_a]$, $S = U - F_t - \mathbf{V} \cdot \triangledown F$. Matching with the outer acoustic solution requires that

$$U \to 0, \quad \mathbf{V} \to 0, \quad P_{\xi} \to 0 \quad \text{as} \quad \xi \to \pm\infty. \tag{3.9}$$

The hydrodynamic motion drives the acoustic motion in the ambient regions by inducing a longitudinal velocity jump. As in WWMP, this key result can be derived by taking the spatial average of the continuity equation in Eq.(3.8) in the (η,ζ) plane, and then integrating the equation with respect to ξ to obtain

$$\overline{U} = \overline{\mathbf{V}\cdot\bigtriangledown F}, \tag{3.10}$$

where the overbar denotes the mentioned average. Inserting the first in Eq.(3.7) into the longitudinal jump in Eq.(2.43), taking the spatial average and using Eq.(3.10), we find

$$\mathcal{J} = [u_a] = -\overline{[[\mathbf{V}]]\cdot\bigtriangledown F} + \overline{[[u]] - q}, \quad [[U]] = \Big([[u]] - \overline{[[u]]}\Big) + \overline{[[\mathbf{V}]]\cdot\bigtriangledown F}. \tag{3.11}$$

Inserting the velocity jumps Eqs.(2.49)–(2.50) into the above equations, we obtain

$$[u_a] = q\Big\{\overline{(1+(\bigtriangledown F)^2)^{\frac{1}{2}}\exp\{\tfrac{1}{2}h_{-\infty}\}} - 1\Big\} - \delta q\Big\{\frac{l\mathcal{D}}{2}\frac{\partial}{\partial t}\overline{(1+(\bigtriangledown F)^2)^{\frac{1}{2}}\exp\{-\tfrac{1}{2}h_{-\infty}\}}$$
$$+\Big(\frac{q}{1+q} + \ln(1+q)\Big)\overline{(1+(\bigtriangledown F)^2)^{\frac{1}{2}}\frac{\tilde{D}}{\tilde{D}t}\exp\{-\tfrac{1}{2}h_{-\infty}\}}\Big\}, \tag{3.12}$$

$$[[U]] = q\Big\{(1+(\bigtriangledown F)^2)^{-\frac{1}{2}}\exp\{\tfrac{1}{2}h_{-\infty}\} - \overline{(1+(\bigtriangledown F)^2)^{\frac{1}{2}}\exp\{\tfrac{1}{2}h_{-\infty}\}}\Big\}$$
$$+\delta\Big\{-\frac{ql\mathcal{D}}{2\kappa}\Big[\bigtriangledown^2 F + \bigtriangledown\cdot\Big(\frac{\kappa}{m}\mathbf{V}^-\Big) + \frac{\partial}{\partial t}(\frac{\kappa}{m}) - \kappa\frac{\partial}{\partial t}\overline{(\frac{\kappa}{m})}\Big]$$
$$+\frac{q\chi}{(1{+}q)m^2}\Big[\frac{\tilde{D}\,\mathbf{V}^-}{\tilde{D}t} + \bigtriangledown F\frac{\tilde{D}U^-}{\tilde{D}t} + \frac{m}{\kappa}\frac{\tilde{D}}{\tilde{D}t}\bigtriangledown F + \Big(G{+}u_{a,t}(0^-,t)\Big)\bigtriangledown F\Big]\cdot\bigtriangledown F$$
$$+\frac{q}{2\kappa}\Bigg[(\mathrm{Pr}{+}1)\bigtriangledown F\cdot\bigtriangledown h_{-\infty} + \Big[\frac{q}{1{+}q} + \ln(1{+}q)\Big]\Big(\frac{\kappa}{m}\frac{\tilde{D}h_{-\infty}}{\tilde{D}t} - \kappa\overline{\frac{\kappa}{m}\frac{\tilde{D}h_{-\infty}}{\tilde{D}t}}\Big)\Bigg]\Bigg\}. \tag{3.13}$$

The transverse velocity jump may be written as

$$[[\mathbf{V}]] = -[[u]]\bigtriangledown f + \delta\Bigg\{\frac{q\chi\kappa}{(1{+}q)m^2}\Big[\frac{\tilde{D}\mathbf{V}^-}{\tilde{D}t} + \bigtriangledown f\frac{\tilde{D}U^-}{\tilde{D}t} + \frac{m}{\kappa}\frac{\tilde{D}}{\tilde{D}t}\bigtriangledown f + \Big(G{+}u_{a,t}(0^-,t)\Big)\bigtriangledown f\Big]$$
$$+\tfrac{1}{2}(\mathrm{Pr}+1)q\bigtriangledown h_{-\infty}\Bigg\}, \tag{3.14}$$

or alternatively as

$$[[\mathbf{V}]] = -[[u]]\bigtriangledown f + \delta\Big\{\mathrm{Pr}\,\frac{\kappa}{m}\Big[\Big[\frac{\partial}{\partial\xi}(\mathbf{V} + U\bigtriangledown f)\Big]\Big] + qPr\frac{m}{\kappa}\bigtriangledown(\frac{\kappa}{m}) + q\frac{\kappa}{2m^2}\bigtriangledown(\frac{m^2}{\kappa})$$
$$+\frac{\kappa}{m^2}\ln(1{+}q)\Big[\frac{\tilde{D}\mathbf{V}^-}{\tilde{D}t} + \bigtriangledown f\frac{\tilde{D}U^-}{\tilde{D}t} + \frac{m}{\kappa}\frac{\tilde{D}}{\tilde{D}t}\bigtriangledown f + \Big(G{+}u_{a,t}(0^-,t)\Big)\bigtriangledown f\Big]\Big\}. \tag{3.15}$$

The jump in the pressure P becomes

$$[[P]] = \Big[R_+\Big(G{+}u_{a,t}(0^+,t)\Big) - R_-\Big(G{+}u_{a,t}(0^-,t)\Big)\Big]F - q\Big[\exp\{h_{-\infty}\}{-}1\Big] - 2m[[u]]$$
$$+\delta\Big\{\frac{qm}{\kappa}\bigtriangledown^2 f + \Big[\frac{\kappa}{m}\frac{\tilde{D}U^-}{\tilde{D}t} + \frac{m}{\kappa}\frac{\tilde{D}}{\tilde{D}t}(\frac{\kappa}{m}) + \Big(G{+}u_{a,t}(0^-,t)\Big)\frac{\kappa}{m}\Big]\ln(1{+}q) - \frac{qm}{2\kappa^2}\bigtriangledown f\cdot\bigtriangledown\kappa$$
$$+\frac{q(\mathrm{Pr}{+}\chi)}{(1{+}q)m}\Big[\frac{\tilde{D}\mathbf{V}^-}{\tilde{D}t} + \bigtriangledown f\frac{\tilde{D}U^-}{\tilde{D}t} + \frac{m}{\kappa}\frac{\tilde{D}}{\tilde{D}t}\bigtriangledown f + \Big(G{+}u_{a,t}(0^-,t)\Big)\bigtriangledown f\Big]\cdot\bigtriangledown f$$

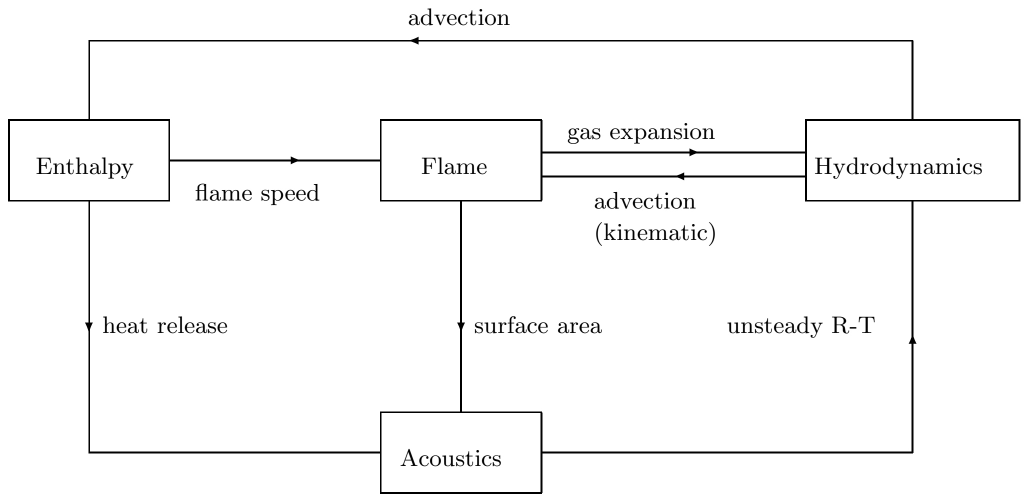

FIGURE 1. Illustration of the couplings among the flame, hydrodynamics, acoustic and enthalpy perturbations.

$$+\frac{qm}{\kappa}(\Pr+1)\,\triangledown f\cdot\triangledown h_{-\infty}\Big\}. \tag{3.16}$$

Note that the local acoustic acceleration, $u_{a,t}(0^{\pm},t)$, plays the same role as gravity G throughout Eqs.(2.49)–(2.51), suggesting that the acoustic field creates an unsteady Rayleigh-Taylor effect, through which it acts on the flame.

The equation governing the advection of enthalpy $h\equiv H$, to $O(\delta)$ accuracy, reads

$$R\Big[\frac{\partial H}{\partial t}+S\frac{\partial H}{\partial \xi}+\mathbf{V}\cdot\triangledown H\Big]+\Big[1+R\mathcal{J}h(\xi)\Big]\frac{\partial H}{\partial \xi}=\delta\Delta H, \tag{3.17}$$

and the initial condition is

$$H\to H_{-\infty}(\eta,\zeta,t-\xi)\quad\text{as}\quad \xi\to-\infty.$$

Eq.(3.17) has to be solved to obtain $h_{-\infty}\equiv H(0,\eta,\zeta,t)$.

The coupling with the flame is completed through the front equation,

$$F_t+\mathbf{V}^-\cdot\triangledown F=U^- -(m-1)+\delta\Big\{\mathrm{M}_a\Gamma-\frac{\kappa}{2m}\Big[\ln(1+q)+\frac{q}{1+q}\Big]\frac{\tilde{D}h_{-\infty}}{\tilde{D}t}\Big\}. \tag{3.18}$$

Equations (3.8), (3.17) and (3.18), coupled to the acoustic equations (3.3) via Eq.(3.6), form an overall interactive system.

4. Discussion and further work

Instability of premixed combustion is a complex phenomenon, in which multi-physical processes occur over a vast range of length scales and yet are intricately coupled. This feature presents a great challenge for DNS. On the other hand, the multi-scale nature of the problem can be exploited mathematically in AEA. This framework has been employed to derive simplified theories describing flame-flow interactions. The theory pertinent to the "corrugate flamelet" regime was given by MM, but spontaneous sound waves emitted by the flame and their back effects on flame were ignored. The latter processes were analyzed by WWMP, leading to a general formulation for flame-acoustic coupling.

The present work extends that of MM and WWMP to include the enthalpy fluctuations in the oncoming mixture. The resulting asymptotically reduced system describes the complicated interactions in flame-acoustic coupling, as illustrated in Fig. 1. The flame-flow interaction is the focus of most studies in combustion, but combustion instability involves further interactions with the acoustic field. The overall coupling was significantly influenced by enthalpy fluctuations. Upstream enthalpy disturbances are advected by the hydrodynamic field. The advection, however, is not passive because enthalpy fluctuations directly influence chemical reactions and therefore modify gas expansion, through which the hydrodynamics is simultaneously influenced. Moreover, the flame motion and enthalpy fluctuations radiate sound waves, whose acceleration creates an unsteady R-T effect to act on the hydrodynamics and ultimately on the flame.

The reduced system remains highly non-linear, and in general has to be solved numerically. Nevertheless, analytical progress may be made in a few special cases to give useful insights into several fundamental processes involving enthalpy disturbances, as will be shown in Part II.

Acknowledgement

We would like to thank Dr. V. Akkerman for helpful comments.

REFERENCES

Baillot, F., Durox, D. & Prud'homme, R. 1992 Experimental and theoretical study of a premixed vibrating flame. *Combust. Flame* **88**(2), 149–168.

Birbaud, A. L., Ducruix, S., Durox, D. & Candel, S. 2008 The nonlinear response of inverted "V" flames to equivalence ratio nonuniformities. *Combust. Flame* **154**, 356–367.

Candel, S. 2002 Combustion dynamics and control: progress and challenges. *Proc. Comb. Inst.* **29**, 1–28.

Cho, J. H. & Lieuwen, T. 2005 Laminar premixed flame response to equivalence ratio oscillations. *Combust. Flame* **140**, 116–129.

Clavin, P. 1994 Premixed combustion and gasdynamics. *Annu. Rev. Fluid Mech.* **26**, 321–352.

Clavin, P., Pelce, P. & He, L. 1990 One-dimensional vibratory instability of planar flames propagating in tubes. *J. Fluid Mech.* **216**, 299–322.

Dowling, A.P. 1999 A kinematic model of a ducted flame. *J. Fluid Mech.* **394**, 51–72.

Dowling, A. P. & Morgans, A. S. 2005 Feedback control of combustion oscillations. *Annu. Rev. Fluid Mech.* **37**, 151–182.

Ducruix, S., Schuller, T., Durox, D. & Candel, S. 2003 Combustion dynamics and instabilities: elementary coupling and driving mechanisms. *J. Prop. Power* **19** (5), 722–734.

Fleifil, M., Annaswamy, A. M., Ghoneim, Z. A. & Ghonmiem, A. F. 1996 Response of a laminar premixed flame to flow oscillations: a kinematic model and thermoacoustic instability results. *Combust. Flame* **106**, 487–510.

Harrje, D. & Reardon, F. 1972 Liquid propellant rocket combustion instability. *NASA Rep.* SP-194.

Harten, A. V., Kapila, A. K. & Matkowsky, B. J. 1984 Acoustic coupling of flames. *SIAM J. App. Math.* **44**, 982–995.

Jones, C. M., LEE, J. G. & Santavicca, D. A. 1999 Closed-loop active control of combustion instabilities using subharmonic secondary fuel injection. *J. Propulsion Power* **15**(4), 584–590.

Langhorne, P. J. 1988 Reheat buzz: an acoustically coupled combustion instability. Part I. Experiment. *J. Fluid Mech.* **193**, 417–443.

Lee, J. G., Kim, K. & Santavicca, D. A. 2000 Measurement of equivalence ratio fluctuation and its effect on heat release during unstable combustion. *Proc. Comb. Inst.* **28**, 415–421.

Lieuwen, T. 2003 Modeling premixed combustion-acoustic wave interactions: a review. *J. Prop. Power* **19**(5), 765–781.

Lieuwen, T. & Zinn, B. T. 1998 The role of equivalence ratio oscillations in driving combustion instabilities in low NO_x gas turbines. *Proc. Comb. Inst.* **27**, 1809–1816.

Markstein, G. H. 1953 Instability phenomena in combustion waves. *Proc. Comb. Inst.* **4**, 44–59.

Matalon, M. & Matkowsky, B. J. 1982 Flames as gasdynamic discontinuities. *J. Fluid Mech.* **124**, 239–259.

Matkowsky, B. J. & Sivashinsky, G. I. 1979 An asymptotic derivation of two models in flame theory associated with the constant density approximation. *SIAM J. Appl. Math.* **37**, 686–699.

McIntosh, A. C. 1991 Pressure disturbances of different length scales interacting with conventional flames. *Comb. Sci. Technol.* **75**, 287–309.

Mcintosh, A. C. 1993 The linearised response of the mass burning rate of a premixed flame to rapid pressure changes. *Comb. Sci. Technol.* **91**, 3329–346.

Pelce, P. & Clavin, P. 1982 Influence of hydrodynamics and diffusion upon the stability limits of laminar premixed flames. *J. Fluid Mech.* **124**, 219–237.

Pelce, P. & Rochwerger, D. 1992 Vibratory instability of cellular flames propagating in tubes. *J. Fluid Mech.* **239**, 293–307.

Poinsot, T.J., Trouve, A.C., Veynante, D.P., Candel, S.M. & Esposito, E.J. 1987 Vortex-driven acoustically coupled combustion instabilities. *J. Fluid Mech.* **177**, 265–292.

Richards, G.A. & Janus, M. 1997 Characterization of oscillations during gas turbine combustion. *ASME paper* 97-GT-244.

Richards, G. A. & Janus, M. & Robey, E. H. 1999 Control of flame oscillations with equivalence ratio modulation. *J. Propulsion Power* **15**(2), 232–240.

Schadow, K. C. & Gutmark, E. 1992 Combustion instability related to vortex shedding in dump combustors and their passive control. *Prog. Energy Comb. Sci.* **18**, 117–132.

Schuller, T. D., Durox, D. & Candel, S. 2003 A unified model for the prediction of flame transfer functions comparisons between conic and V-flame dynamics. *Combust. Flame* **134**, 21–34.

Searby, G. & Rochwerger, D. 1991 A parametric acoustic instability in premixed flames. *J. Fluid Mech.* **231**, 529–543.

Shin, W. P, Lee, J. & Santavicca, D. 1996 Stability and emissions characteristics of a lean gas turbine combustor. *Proc. Comb. Inst.* **26**, 2711.

Wu, X. & Law, C.K. 2008 Flame-acoustic resonance initiated by vortical disturbances. *J. Fluid Mech.* (submitted).

Wu, X. Wang, M., Moin, P. & Peters, N. 2003 Combustion instability due to the nonlinear interaction between sound and flame. *J. Fluid Mech.* **497**, 23–53.

Yu, K. H., Trouve, A. & Daily, J.W. 1991 Low-frequency pressure oscillations in a model ramjet combustor. *F. Fluid Mech.* **232**, 47–72.

Zimmer, L. & Tachibana, S. 2007 Laser induced plasma spectroscopy for local equivalence ratio measuremenrs in an oscillating combustion environment. *Proc. Comb. Inst.* **31**, 737–745.